6th International Electronic Conference on Medicinal Chemistry

1-30 November 2020

sciforum.net/conference/ECMC2020

sponsored by pharmaceuticals

Prevention of the probe hole clogging up during administration of nano Ag preparations in animal models of GI diseases

Krzysztof Siczek [1,*], Przemyslaw Kubiak [2], and Justyn Ochocki [3]

[1] Department of Vehicles and Fundamentals of Machine Design, Lodz University of Technology, Poland, Stefanowskiego Str. 1/15, 90-537 Lodz, Poland;

[2] Institute of Vehicles and Construction Machinery Engineering, Warsaw University of Technology, Poland, Narbutta Str. 84, 02-524 Warsaw, Poland;

[3] Department of Bioinorganic Chemistry, Chair of Medicinal Chemistry, Medical University of Lodz, Muszynskiego Str. 1, 90-151 Lodz, Poland.

Lodz University of Technology

Warsaw University of Technology

MEDICAL UNIVERSITY OF LODZ

* Corresponding author: krzysztof.siczek@p.lodz.pl

Prevention of the probe hole clogging up during administration of nano Ag preparations in animal models of GI diseases

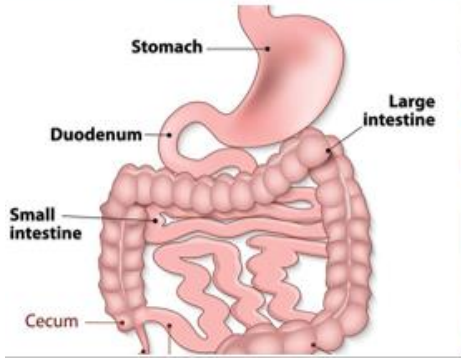

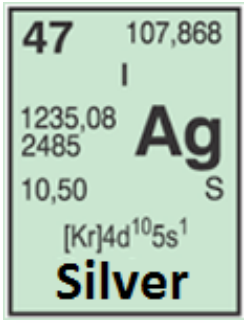

Abstract:

The present study concerns the resistance to motion of syringe plunger against syringe barrel during intragastrical administration of silver preparations into mice models of Gastrointestinal Diseases. The mathematical model of drug flow in the syringe barrel-hub-needle assembly was elaborated and presented. The effect of geometrical parameters of the mentioned assembly affecting the resistance to motion was profoundly investigated. The resistance to motion during administration of silver preparation depended mainly on the needle hole diameters and hub hole. The form of silver preparation and length of needle only slightly affected the resistance to motion. The important role of albumin in prevention of Ag nanoparticles agglomeration was found.

Keywords: gastrointestinal tract, animal model, Ag preparations, anti-clogging

1. Introduction

Infectious, autoimmune, and physiological states often occur in the small and large intestines.

Inflammation of the intestines (enterocolitis) and the other diseases of them can be accompanied by by vomiting, diarrhea, constipation, and altered bowel habits, such as with blood in stool.

Acute and chronic conditions affecting the bowels include infectious diarrhea and mesenteric ischaemia.

The constipation is mainly casues by the faecal impaction and bowel obstruction, in turn resulting from ileus, intussusception, volvulus.

Inflammatory bowel diseases of unknown etiology, such as Crohn's disease or ulcerative colitis, affect the intestines and other parts of the gastrointestinal tract.

Other causes of illness include intestinal pseudo-obstruction, and necrotizing enterocolitis.

Colledge, Walker, Ralston, & Davidson. (2010). Davidson's principles and practice of medicine. (21st ed. / the editors, Nicki R. Colledge, Brian R. Walker, Stuart H. Ralston ; illustrated by Robert Britton.). Churchill Livingstone/Elsevier, 850–862, 895–903

1.1. GI diseases localization

Small intestine

- Inflammation of the small intestine (enteritis): duodenitis, jejunitis, ileitis.
- Peptic ulcers in the duodenum.
- Chronic diseases of malabsorption: the autoimmune coeliac disease, infective Tropical sprue, and congenital or surgical short bowel syndrome.
- Curling's ulcer, blind loop syndrome, Milroy disease and Whipple's disease.
- Gastrointestinal stromal tumours, lipomas, hamartomas, carcinoid syndromes.

Large intestine

- Appendicitis caused by inflammation of the appendix.
- Generalised inflammation of the large intestine (colitis), and pseudomembranous colitis caused by the bacteria Clostridium difficile.
- Diverticulitis caused by abdominal pain from outpouchings affecting the colon.
- Functional diseases: irritable bowel syndrome and intestinal pseudo-obstruction.
- Constipation result from lifestyle factors,
- Impaction of a rigid stool in the rectum,
- Hirschprung's disease in neonates.

Colledge, Walker, Ralston, & Davidson. (2010). Davidson's principles and practice of medicine. (21st ed. / the editors, Nicki R. Colledge, Brian R. Walker, Stuart H. Ralston ; illustrated by Robert Britton.). Churchill Livingstone/Elsevier, 879-887, 913–915

1.1. GI diseases localization

Rectum and anus

Older adults are often affected by:

- Hemorrhoids, vascular outpouchings of skin, and pruritus ani (anal itchiness);
- Anal cancer associated with ulcerative colitis or with sexually transmitted infections like HIV;
- Inflammation of the rectum (proctitis) resulted from radiation damage during radiotherapy to further sites such as the prostate;
- Faecal incontinence caused by mechanical and neurological problems;
- Encopresis - faecal incontinence accompanied with a lack of voluntary voiding ability;

Pain on passing stool due to anal abscesses, small inflamed nodules, anal fissures, and anal fistulas.

Colledge, Walker, Ralston, & Davidson. (2010). Davidson's principles and practice of medicine. (21st ed. / the editors, Nicki R. Colledge, Brian R. Walker, Stuart H. Ralston ; illustrated by Robert Britton.). Churchill Livingstone/Elsevier, 915–916

1.2. The use of Ag in some GI and associated diseases

Various structures with Ag, Cu and other metals can be utilized as future drugs against GI diseases.

Siczek K, Zatorski H, Fichna J. Silver and other metals in the treatment of gastrointestinal diseases. Curr Med Chem. 2015;22(32):3695-706. doi: 10.2174/0929867322666151001121439

There are some studies examining the toxic effects of AgNPs on intestinal bacteria, particularly, on bactericidal toxicity and AgNP-specific mechanisms.

Li, J., Tang, M., Xue, Y. (2018). Review of the effects of sliver nanoparticle exposure on gut bacteria. Journal of Applied Toxicology. 39. 10.1002/jat.3729..

The synthesis, structure, evaluation of the cytotoxic activity of Ag(I) complexes with miconazole medical agent was reported. The complexes of Ag(I) ions with the biologically active ligand miconazole inhibited the growth of HepG2 cancer cells.

Stryjska, K., Radko, L., Chęcińska, L., Lusz, J., Posyniak, A., Ochocki, J., Synthesis, spectroscopy, light stability and biological activity of silver(I) complexes of miconazole drug and selected counter-ions. X-ray crystal structure of [Ag(MCZ)2NO3], [Ag(MCZ)2ClO4], Int. J. Mol. Sci. 2020, 21, 3629; doi:10.3390/ijms21103629

The cytotoxicity of Ag(I) complexes based on metronidazole medical agent were assessed against human-derived hepatic carcinoma cells (Hep-G2) and showed modified pharmacological and toxicological potential.

Radko, L., Stypuła-Trębas, S., Posyniak, A., Żyro, D., Ochocki, J., Silver(I) Complexes of the Pharmaceutical Agents Metronidazole and 4-Hydroxymethylpyridine: Comparison of Cytotoxic Profile for Potential Clinical Application, Molecules 2019, 24(10), 1949; https://www.mdpi.com/1420-3049/24/10/1949

Ag(I)-metronidazole complex, $[Ag(MTZ)_2NO_3]$ (MTZ, 2-(2-methyl-5-nitro-1H-imidazol-1- yl)ethanol) was clinically assessed in the treatment of ocular rosacea in an effort to introduce an alternative method of acne rosacea treatment.

Waszczykowska, A., Jurowski, P., Żyro, D., Ochocki, J., Effect of Treatment of Silver(I) Complex of Metronidazole on Ocular Rosacea. Design and Formulation of New Silver Drug With Potent Antimicrobal Activity, Journal of Trace Elements in Medicine and Biology, https://doi.org/10.1016/j.jtemb.2020.126531 020) 126531

2. Animal Models of Gastrointestinal Diseases

Some animal models relates to the upper gastrointestinal disorders involving the esophagus, stomach, and small intestine and lower gastrointestinal disorders that focus on the colon. There were not evaluated models based on surgical or other non-pharmacological interventions for treatment.

Johnson AC, Greenwood-Van Meerveld B. Critical Evaluation of Animal Models of Gastrointestinal Disorders. Handb Exp Pharmacol. 2017;239:289-317. doi: 10.1007/164_2016_120

Studies in rats and mices address the processes, such as regulation of mucosal proliferation, apoptosis, transport, and digestive enzyme expression, and allow exogenous or genetic manipulation of growth factors and their receptors (e.g., glucagon-like peptide 2, growth hormone, insulin-like growth factor 1, epidermal growth factor, keratinocyte growth factor). The greater size of rats, and young pigs, facilitates testing surgical procedures and nutritional interventions (e.g., PN, milk diets, long-/short-chain lipids, pre- and probiotics). Newborn pigs (preterm or term) and weanling rats provide insights into the developmental aspects of treatment for SBS in infants owing to their immature intestines.

Sangild PT, Ney DM, Sigalet DL, Vegge A, Burrin D. Animal models of gastrointestinal and liver diseases. Animal models of infant short bowel syndrome: translational relevance and challenges. Am J Physiol Gastrointest Liver Physiol. 2014 Dec 15;307(12):G1147-68. doi: 10.1152/ajpgi.00088.2014

2.1. Animal Models of IBD

Inflammatory bowel disease (IBD) models include 66 animal models, like chemically induced, cell-transfer, congenial mutant, and genetically engineered ones.

Mizoguchi A. Animal models of inflammatory bowel disease. Prog Mol Biol Transl Sci. 2012;105:263-320. doi: 10.1016/B978-0-12-394596-9.00009-3

There were identified:

20 kinds of genetically engineered mouse models carrying the susceptibility genes identified in human IBD,

74 kinds of genetically engineered mouse models spontaneously developing intestinal inflammation.

Mizoguchi A, Takeuchi T, Himuro H, Okada T, Mizoguchi E. Genetically engineered mouse models for studying inflammatory bowel disease. J Pathol. 2016 Jan;238(2):205-19. doi: 10.1002/path.4640

IBD can be induced in mice by dextran sulfate sodium (DSS) or by a 2,4,6-trinitrobenzene sulfonic acid (TNBS) ethanol enema, evoking immune responses and colitis. To evaluate the effects of TNBS on inflammasome activation, caspase-1 knockout (KO) mice can be used.

Oh SY, Cho KA, Kang JL, Kim KH, Woo SY. Comparison of experimental mouse models of inflammatory bowel disease. Int J Mol Med. 2014 Feb;33(2):333-40. doi: 10.3892/ijmm.2013.1569

DSS-Induced Acute Colitis model can be realized in rats.

Martin JC, Bériou G, Josien R. Dextran Sulfate Sodium (DSS)-Induced Acute Colitis in the Rat. Methods Mol Biol. 2016;1371:197-203. doi: 10.1007/978-1-4939-3139-2_12

2.2. Animal Models of gastrointestinal cancer

A novel mouse model of IBD-colorectal cancer progression in which disrupted immune regulation, mTOR-Stat3 signaling, and epithelial hyperproliferation were integrated and simultaneously linked to the development of malignancy.

Deng L, Zhou JF, Sellers RS, Li JF, Nguyen AV, Wang Y, Orlofsky A, Liu Q, Hume DA, Pollard JW, Augenlicht L, Lin EY. A novel mouse model of inflammatory bowel disease links mammalian target of rapamycin-dependent hyperproliferation of colonic epithelium to inflammation-associated tumorigenesis. Am J Pathol. 2010 Feb;176(2):952-67. doi: 10.2353/ajpath.2010.090622

Mouse models of gastrointestinal tumors include:

- models for familial adenomatous polyposis (Apc mutant mice; modifier genes of Apc intestinal polyposis; stabilizing beta-catenin mutant mice);
- models for colon cancer (mouse models for hereditary non-polyposis colon cancer; additional mutations in Apc mutant mice; models with mutations in other genes; models for colon cancer associated with inflammatory bowel diseases);
- mouse models for gastric cancer.

Taketo MM. Mouse models of gastrointestinal tumors. Cancer Sci. 2006 May;97(5):355-61. doi: 10.1111/j.1349-7006.2006.00190.x

Pharmacological models of chronic dysmotility can be realized in aged rats.

Dalziel JE, Young W, Bercik P, Spencer NJ, Ryan LJ, Dunstan KE, Lloyd-West CM, Gopal PK, Haggarty NW, Roy NC. Tracking gastrointestinal transit of solids in aged rats as pharmacological models of chronic dysmotility. Neurogastroenterol Motil. 2016 Aug;28(8):1241-51. doi: 10.1111/nmo.12824

2.3. Animal Models for Metabolism Studies

Animal models, particularly rats and mice, are extensively used for studies aimed to understand the consequences of diet quality on weight gain and health.

Chalvon-Demersay T, Blachier F, Tomé D, Blais A. Animal Models for the Study of the Relationships between Diet and Obesity: A Focus on Dietary Protein and Estrogen Deficiency. Front Nutr. 2017 Mar 20;4:5. doi: 10.3389/fnut.2017.00005.

Results of rodent studies are usually confirmed in pigs before extrapolating them to humans. This applies to gastrointestinal and metabolism studies due to similarities between pig and human physiology.

Intrauterine growth retarded (IUGR) pig neonate is a good model for the better understanding of the IUGR syndrome in humans.

In pigs, the induction of IUGR syndrome may include the maternal diet intervention, the dexamethasone treatment or temporary reduction of the blood supply.

In pigs, like in humans, about 8% of neonates develop IUGR syndrome spontaneously.

The pigs provide very good animal models for the studies on human gastrointestinal tract structure and on the function development in IUGR syndrome.

Ferenc, K., Pietrzak, P., Godlewski, M., Piwowarski, J., Kilianczyk, R., Guilloteau, P., Zabielski, R. (2014). Intrauterine growth retarded piglet as a model for humans - Studies on the perinatal development of the gut structure and function. Reproductive biology. 14. 51-60. 10.1016/j.repbio.2014.01.005.

2.4. Agglomeration of Silver Nanoparticles

During studies on anti-inflammatory properties of silver nanoparticle suspensions in experimental mousy colitis clogging up of the needle hole and hub hole were sometimes observed during administration of such colloidal suspension intragastrically into mice using syringe with needle (probe). Such problems, although rarely occurring, related to the agglomeration process of such nanoparticles and were affected by accuracy of the test sample preparation.

Siczek, K., Zatorski, H., Chmielowiec-Korzeniowska, A., Pulit-Prociak, J., Śmiech, M., Kordek, R., Fichna, J. (2017). Synthesis and evaluation of anti-inflammatory properties of silver nanoparticle suspensions in experimental colitis in mice. Chemical Biology and Drug Design, 89(4). https://doi.org/10.1111/cbdd.12876

Albumin is an excellent capping agent to minimize Ag-NPs agglomeration.

Valenti, L.E., Giacomelli, C.E. Stability of silver nanoparticles: agglomeration and oxidation in biological relevant conditions. J Nanopart Res 19, 156 (2017). https://doi.org/10.1007/s11051-017-3860-4

3. Drug flow in the syringe barrel-hub-needle assembly

3.1. Flow model

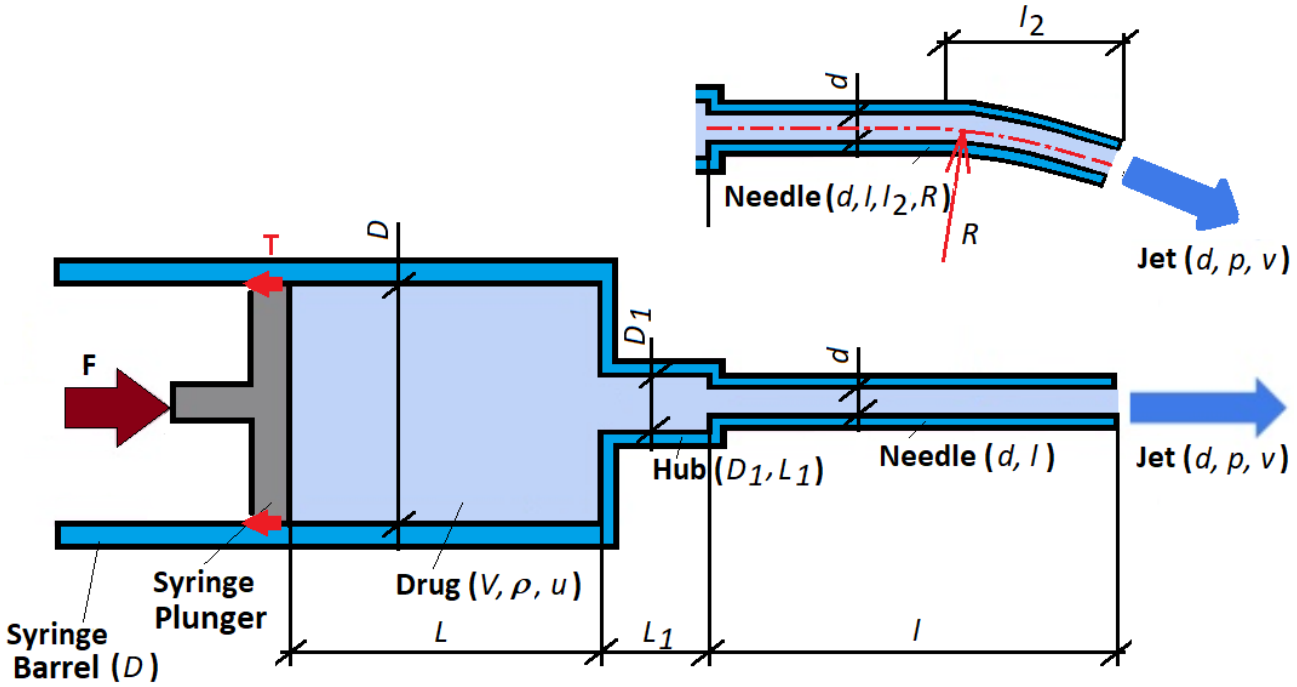

Fig. 1. Geometrical model of the drug-plunger-barrel-hub-needle assembly

3.1. Flow model

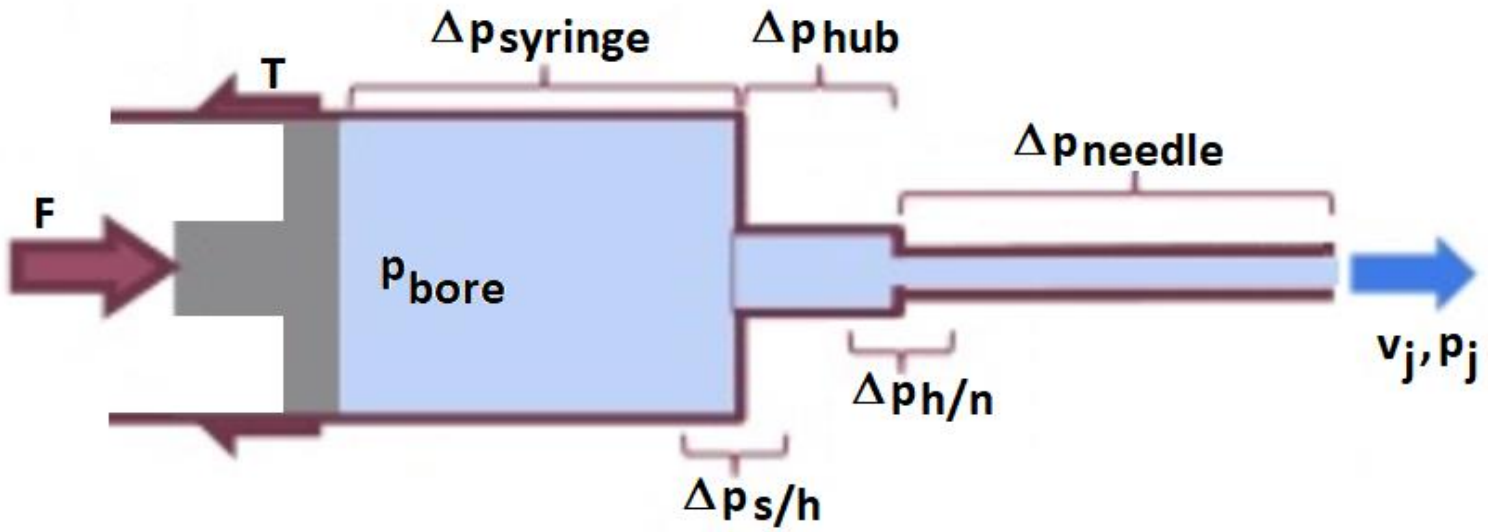

Fig. 2. Boundary conditions in the drug-plunger-barrel-hub-needle assembly model

3.2. Properties of nanofluid

At T = 27 °C, the density of ρ_{water}= 998.2 kg·m^{-3}, of ρ_{AgNPs}= 10490 kg·m^{-3}.

Sadripour, S., Chamkha, A.J. The effect of nanoparticle morphology on heat transfer and entropygeneration of supported nanofluids in a heat sink solar collector, Thermal Science and Engineering Progress 9 (2019) 266–280, https://doi.org/10.1016/j.tsep.2018.12.002

The density of nanofluid is obtained from equation (hereused to the case of water solution of BSA with Ag nanoparticles or nanowires)

$$\rho_{nf} = \rho_{bf} \cdot (1 - \emptyset) + \rho_{NP} \cdot \emptyset$$

Selvam, C., Mohan Lal, D. & Harish, S. Thermophysical properties of ethylene glycol-water mixture containing silver nanoparticles. J Mech Sci Technol 30, 1271–1279 (2016). https://doi.org/10.1007/s12206-016-0231-5

For the other case was used equation

$$\rho_{nf} = \rho_{bf} \cdot (1 + 4.1 \cdot 10^{-2} \cdot \emptyset + 1.2 \cdot 10^{-3} \cdot \emptyset \cdot T + 4.276 \cdot 10^{-5} \cdot T)$$

Selvam, C., Mohan Lal, D. & Harish, S. Thermophysical properties of ethylene glycol-water mixture containing silver nanoparticles. J Mech Sci Technol 30, 1271–1279 (2016). https://doi.org/10.1007/s12206-016-0231-5

$$\emptyset = C_{Ag-water}/\rho_{Ag}$$

$C_{Ag-water}$= 0.5 kg_{Ag}·m^{-3} – amount of Ag NPs in 1 m^3 of water

Siczek, K., Zatorski, H., Chmielowiec-Korzeniowska, A., Pulit-Prociak, J., Śmiech, M., Kordek, R., Fichna, J. (2017). Synthesis and evaluation of anti-inflammatory properties of silver nanoparticle suspensions in experimental colitis in mice. Chemical Biology and Drug Design, 89(4). https://doi.org/10.1111/cbdd.12876

Obtained $\emptyset = 4.77 \cdot 10^{-5}$ – volume fraction of Ag NPs in water

3.2. Properties of nanofluid

At T = 27 °C:

The viscosity of water η_{bf} = 0.000851Pa·s

The viscosity of nanofluid with almost spherical Ag NPs is obtained from equation

$$\eta_{nf} = \eta_{bf} \cdot (1.0511 - 0.9641 \cdot \emptyset + 0.4390 \cdot \emptyset \cdot T + 4 \cdot 10^{-4} \cdot T)$$

Sadripour, S., Chamkha, A.J. The effect of nanoparticle morphology on heat transfer and entropygeneration of supported nanofluids in a heat sink solar collector, Thermal Science and Engineering Progress 9 (2019) 266–280, https://doi.org/10.1016/j.tsep.2018.12.002

The viscosity of nanofluid containing Ag nanowires is obtained from Einstein equation

$$\eta_{nf} = \eta_{bf} \cdot (1 + 2.5 \cdot \emptyset)$$

Sadripour, S., Chamkha, A.J. The effect of nanoparticle morphology on heat transfer and entropygeneration of supported nanofluids in a heat sink solar collector, Thermal Science and Engineering Progress 9 (2019) 266–280, https://doi.org/10.1016/j.tsep.2018.12.002

3.2. Properties of nanofluid

At T = 27 °C, the density of water solution of Bovine Serum Albumine (BSA) ρ_{BSA}

Singh, M., Chand, H., Gupta, K.C., The Studies of Density, ApparentMolar Volume, and Viscosity of Bovine Serum Albumin, Egg Albumin, and Lysozyme in Aqueous and RbI, CsI, and DTAB Aqueous Solutions at 303.15 K, Chemistry& Biodiversity, Vol. 2 (2005), 809-824

$$\rho_{BSA} = \rho^0_{BSA} + S_d \cdot m$$

where: $\rho^0_{BSA} = 0.9964 g/cm^3, S_d = 0.2764 \cdot 10^3 g^2/cm^3 \cdot mol$

Maximum molality of water solution of BSA https://www.sigmaaldrich.com/catalog/product/sigma/a2058?lang=pl&region=PL

$$m = \frac{40\ \frac{mg_{BSA}}{ml_{H20}}}{66000 Da_{BSA}} = \frac{\frac{40}{1}\frac{mg_{BSA}}{g_{H20}}}{66000\ \frac{g}{mol_{BSA}}} = 0.6 \cdot 10^{-6} mol/g$$

The viscosity of Bovine Serum Albumine$\eta_{BSA}$is estimated from equation

Singh, M., Chand, H., Gupta, K.C., The Studies of Density, ApparentMolar Volume, and Viscosity of Bovine Serum Albumin, Egg Albumin, and Lysozyme in Aqueous and RbI, CsI, and DTAB Aqueous Solutions at 303.15 K, Chemistry& Biodiversity, Vol. 2 (2005), 809-824

$$\left(\frac{\eta_{BSA-water}}{\eta_{water}} - 1\right) = (B + D \cdot m) \cdot m$$

where: $B = -32.58 \cdot 10^3 g/cm^3, D = 22606 \cdot 10^3 g/cm^3$

3.3. Resistance to drug flow

Equation of flow continuity

$$\frac{\pi d^2}{4} v_j = \frac{\pi D^2}{4} v_1 = \frac{\pi D^2}{4} \frac{dx_1}{dt}; \quad \frac{dx_1}{dt}(t = 0) \approx 0$$

Coefficient of resistance to laminar flow

$$f = \frac{64}{R_e}$$

Reynolds numer for syringe barrel Re_s, hub Re_h, needle Re_n, respectively

$$Re_s = \frac{\rho \cdot D}{\eta} \cdot \frac{v_1 + v_j}{2}; \qquad Re_h = \frac{\rho \cdot D_1}{\eta} \cdot \frac{v_1 + v_j}{2}; \qquad Re_n = \frac{\rho \cdot d}{\eta} \cdot \frac{v_1 + v_j}{2}.$$

η - dynamic viscosity of fluid, D= 0.01 m - inner diameter of syringe barrel, L= 0.05 m – barrel length, v – speed of fluid

3.3. Resistance to drug flow

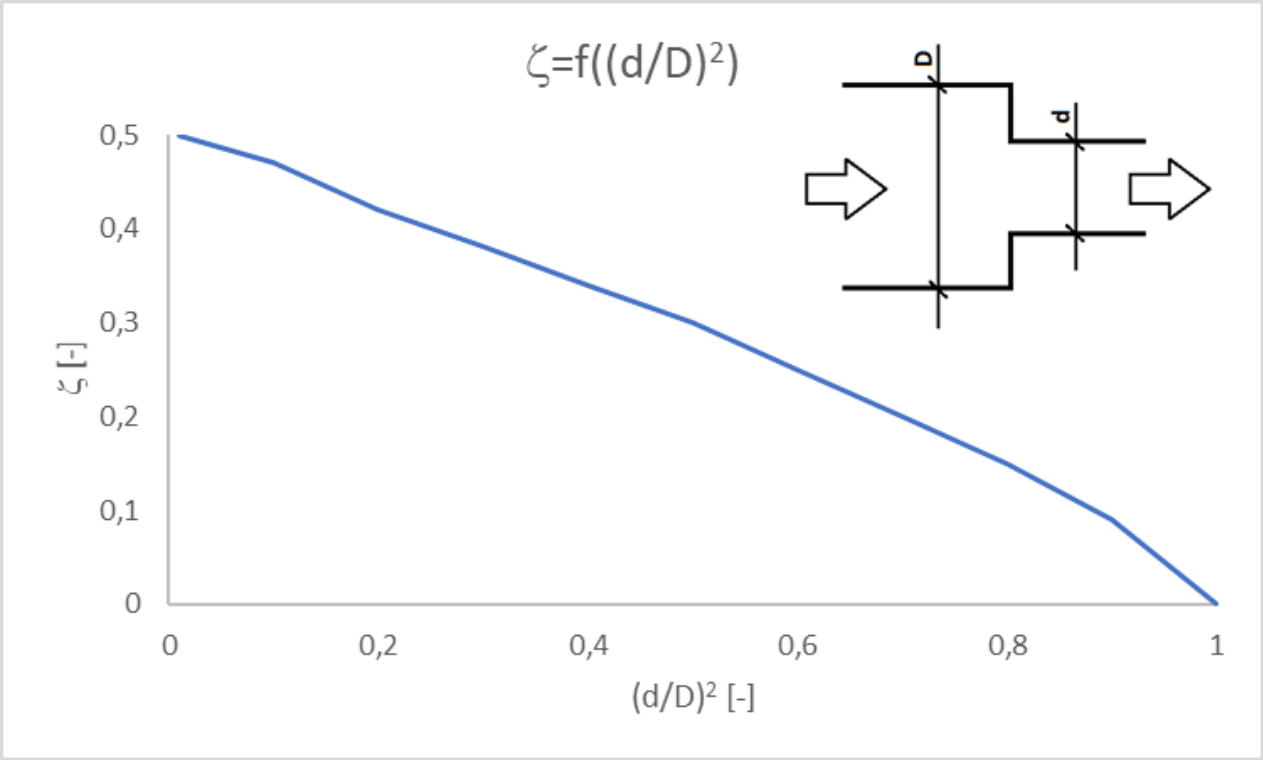

Fig. 3. The course of the coefficient of local resistance to flow versus diameter ratio for the flow from pipe of greater diameter to the pipe of smaller diameter

Based on data from: Idel'chik, I.E., Handbook of hydraulic Resistance. Coefficients of Local Resistance and of Friction. Gosudarstvennoe Energeticheskoe Izdatel'stvo Moskva-Leningrad 1960. Translated from Russian. Israel Program for Scientific Translations, Jerusalem 1966.

3.3. Resistance to drug flow

Table 1. The coefficient of local resistance to flow versus diameter/curvature radius and angle δ

δ [deg]	r/d [-]	1	2	4	6	10
15		0.03	0.03	0.03	0.03	0.03
22.5		0.045	0.045	0.045	0.045	0.045
45		0.14	0.09	0.08	0.075	0.07
60		0.19	0.12	0.10	0.09	0.07
90		0.21	0.14	0.11	0.09	0.08

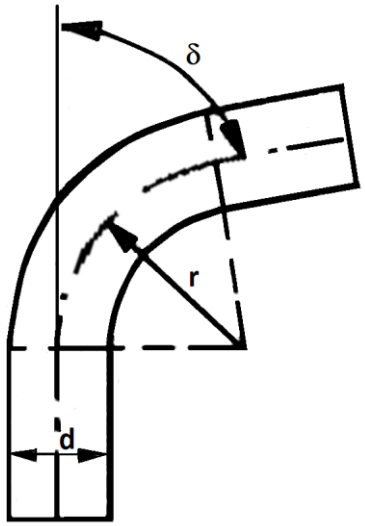

During the present analysis of the case of curved needle, the following values were assumed: r/d =10, δ = 45°, which related to ζ = 0.07

Idel'chik, I.E., Handbook of hydraulic Resistance. Coefficients of Local Resistance and of Friction. Gosudarstvennoe Energeticheskoe Izdatel'stvo Moskva-Leningrad 1960. Translated from Russian. Israel Program for Scientific Translations, Jerusalem 1966.

3.3. Resistance to drug flow

Equation of stopper motion

$$M \cdot \frac{d^2 x_1}{dt^2} = F - T - p_{bore} \cdot \pi \cdot \frac{\pi D^2}{4}$$

M = 0.01 kg – mass of syringe plunger

D = 0.01 m – mass of syringe barrel

F = 3 N – maximal value of the force from the hand action on syringe plunger

Friction force between syringe plunger and syringe barrel

$$T = \mu \cdot p_{poly-poly} \cdot \pi \cdot D \cdot k$$

$p_{poly-poly}$ = 100000 Pa – contact pressure in polypropylene-polypropylene contact between syringe plunger and syringe barrel

μ = 0. 44 - kinematic friction coefficient in polypropylene-polypropylene contact

Typical Engineering Properties of Polypropylene, https://www.ineos.com/globalassets/ineos-group/businesses/ineos-olefins-and-polymers-usa/products/technical-information--patents/ineos-engineering-properties-of-pp.pdf

3.3. Resistance to drug flow

Bernoulli Equation

$$p_{bore} = p_j + \frac{v_j^2 - v_1^2}{2} \cdot \rho + \frac{\rho}{2} \cdot \left[\frac{64}{Re_s} \cdot \frac{L}{D} \cdot \left(\frac{v_1 + v_j}{2} \right)^2 + \zeta_{s/h} \cdot \left(\frac{v_1 + v_j}{2} \right)^2 + \frac{64}{Re_h} \cdot \frac{L_1}{D_1} \cdot \left(\frac{v_1 + v_j}{2} \right)^2 + \zeta_{h/n} \cdot \left(\frac{v_1 + v_j}{2} \right)^2 + \frac{64}{Re_n} \cdot \frac{l}{d} \cdot \left(\frac{v_1 + v_j}{2} \right)^2 \right]$$

$\zeta_{s/h}$- the coefficient of localresistance to flow between syringe barrel and hub

$\zeta_{h/n}$- the coefficient of localresistance to flow between hub and needle

p_j = 0 Pa – outlet pressure

4. Results and discussion

Table 2. Densities and dynamic viscosities of different drug fluid and nanofluid.

Base fluid	Nanoparticles	Density	Viscosity
		kg/m^3	Pa·s
Water	-	996.5	0.000851
Water	Ag NPs	1001	0.000903
Water	Ag Nanowires	1001	0.000850
Water	BSA	996.8	0.000833
Water+BSA	Ag NPs	997.2	0.000940
Water+BSA	Ag Nanowires	997.2	0.000833

The form of Ag in solutions did not affect neither density nor viscosity. The addition of Ag increased slightly density. The addition of Ag NPs increased dynamic viscosities of drug fluid base form, however addition of Ag nanowires practically did not change the dynamic viscosities of drug fluid.

4. Results and discussion

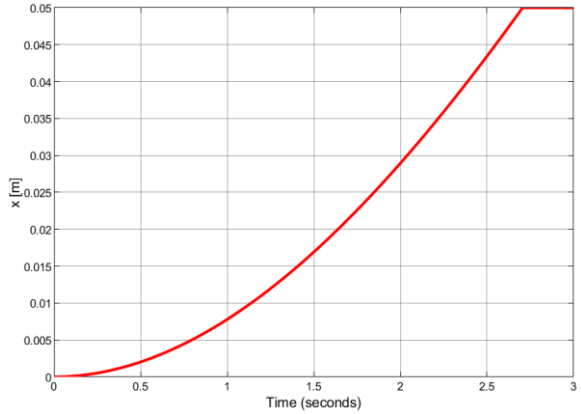

Fig. 4. Plunger displacement vs. time for water, d = 1 mm, l = 5 cm, D_1 = 1.5 mm

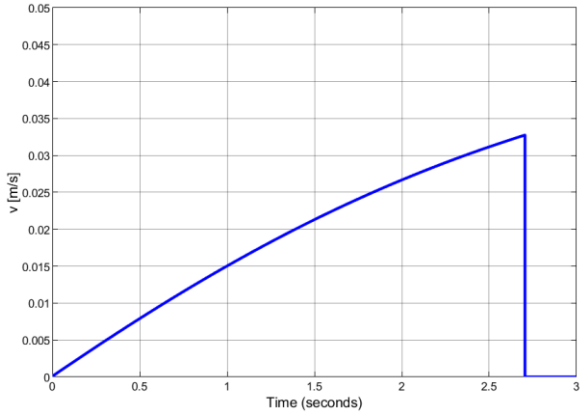

Fig. 5. Plunger speed vs. time for water, d = 1 mm, l = 5 cm, D_1 = 1.5 mm

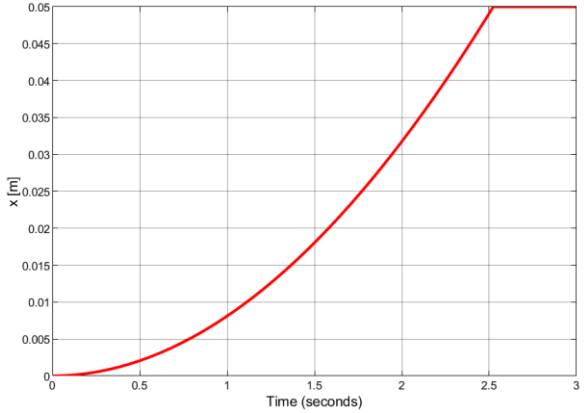

Fig. 6. Plunger displacement vs. time for water, d = 1.5 mm, l = 5 mm, D_1 = 2 mm

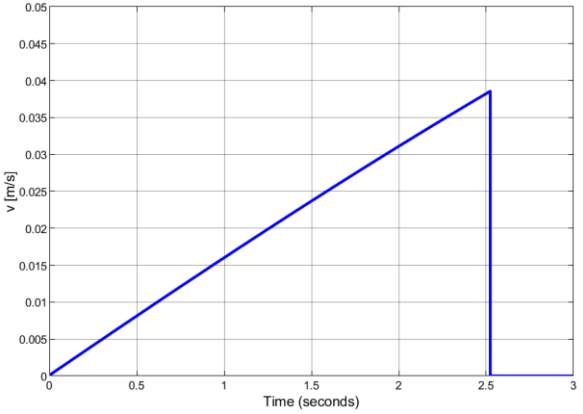

Fig. 7. Plunger speed vs. time for water, d = 1.5 mm, l = 5 mm, D_1 = 2 mm

Obtained courses of the plunger displacement vs time and its speed vs. time were close comparing cases of:
- water and water with Ag NPs or Ag nanowires for the same values of d, D1 and l,
- water and water with BSA with/without Ag NPs or Ag nanowires for the same values of d, D1 and l,
- the same values of d, D_1 and values of l differing by 50 %.

4. Results and discussion

Table 3. Time and speed of syringe plunger in the end of its displacement for water, and water + Ag NPs, d = 1 mm, l = 5 cm, D1 = 1.5 mm

Medium	Time [s]	Speed [m/s]
water	2.7051	0.03482
Water + Ag NPs	2.7135	0.03452
Water + Ag Nanowires	2.7055	0.03480

Table 4. Time and speed of syringe plunger in the end of its displacement for water, and water + Ag NPs, d = 1.5 mm, l = 5 cm, D1 = 2 mm

Medium	Time [s]	Speed [m/s]
water	2.5235	0.04504
Water + Ag NPs	2.5250	0.04494
Water + Ag Nanowires	2.5230	0.04503

Table 5. Time and speed of syringe plunger in the end of its displacement for water, and water + Ag NPs, d = 1.5 mm, l = 7.5 cm, D1 = 2 mm

Medium	Time [s]	Speed [m/s]
water	2.5349	0.04435
Water + Ag NPs	2.5372	0.04422
Water + Ag Nanowires	2.5350	0.004435

The enhancement of the needle hole diameter by 50% decreased time of the plunger motion by 7% and increased the speed in the end of the motion by 30%. Increasing the needle length by 50% increased the time of the motion by 0.4% and decreased the speed in the end of the motion by 1.5%. Addition of Ag NPs increased the time of the motion by 0.3 % and decreased the speed in the end of the motion by 0.8%. Addition of Ag nanowires did not affect them.

Results and discussion

Table 6. Time and speed of syringe plunger in the end of its displacement for water, and water + Ag NPs, d = 1 mm, l = 5 cm, D1 = 1.5 mm

Medium	Time [s]	Speed [m/s]
Water + BSA	2.7023	0.03492
Water + BSA + Ag NPs	2.7180	0.03439
Water + BSA + Ag Nanowires	2.7013	0.03497

Table 7. Time and speed of syringe plunger in the end of its displacement for water, and water + Ag NPs, d = 1.5 mm, l = 5 cm, D1 = 2 mm

Medium	Time [s]	Speed [m/s]
Water + BSA	2.5230	0.04507
Water + BSA + Ag NPs	2.5260	0.04488
Water + Ag Nanowires	2.5230	0.04507

Table 8. Time and speed of syringe plunger in the end of its displacement for water, and water + Ag NPs, d = 1.5 mm, l = 7.5 cm, D1 = 2 mm

Medium	Time [s]	Speed [m/s]
water	2.5341	0.04440
Water + BSA + Ag NPs	2.5380	0.04413
Water + BSA + Ag Nanowires	2.5340	0.04440

The addition of BSA into water decreased time of plunger motion by 0.1% and increased speed in the end of the motion by 0.3%. The enhancement of a needle hole diameter by 50% decreased time of plunger motion by 7% and increased the speed in the end of the motion by 30%. Increasing the needle length by 50% increased time of the motion by 0.4% and decreased the speed in the end of the motion by 1.5%. Addition of Ag NPs increased the time of motion by 0.3 % and decreased the speed in the end of the motion by 0.8%. Addition of Ag nanowires did not affect them.

4. Results and discussion

Table 8. Time and speed of syringe plunger in the end of its displacement for water, and water + Ag NPs, d = 1.5 mm, l = 7.5 cm, D1 = 2 mm

Medium	Time [s]	Speed [m/s]
Water + BSA	2.5340	0.04437
Water + BSA + Ag NPs	2.5390	0.04410
Water + BSA + Ag Nanowires	2.5345	0.04437

The introduction of curvature to the needle only slightly affected time of syringe plunger motion and its speed in the end of this kind of motion.

5. Conclusions

1. The resistance to motion during administration of silver preparation are mainly affected by the needle hole diameter and related to it the hub hole diameter.
2. The form of silver preparation practically does not affect the resistance to motion of syringe plunger against syringe barrel.
3. The change of 50% in diameter results in only slight change of resistance to motion of syringe plunger against syringe barrel.
4. The addition of BSA only slightly affects the resistance to motion of plunger but can prevent or delay agglomeration process of silver preparation in water solution.
5. The introduction of curvature to the needle only slightly affects the resistance to motion of syringe plunger against syringe barrel.

Acknowledgments

Thank You, very much, for Your attention!

The research has been partially financially supported (JO) by the National Science Centre in Poland (chemical part: grant UMO-2014/15/B/NZ7/00944)